GEOCHEMICAL ASPECTS OF THE CARBONATION OF MAGNESIUM SILICATES IN AN AQUEOUS MEDIUM

George D. Guthrie, Jr. (gguthrie@lanl.gov 505-665-6340)
J. William Carey (bcarey@lanl.gov 505-667-5540)
Deborah Bergfeld (debberrg@lanl.gov 505-667-1812)
Darrin Byler (dbyler@lanl.gov 505-665-9562)
Steve Chipera (chipera@lanl.gov 505-667-1110)
Hans-Joachim Ziock (ziock@lanl.gov 505-667-7265)
Hydrology, Geochemistry, & Geology
Los Alamos National Laboratory
Los Alamos, NM 87545

Klaus Lackner (ksl@lanl.gov 505-667-5694)
Theoretical Division, Los Alamos National Laboratory, Los Alamos, NM
and Columbia University, New York, NY

KEYWORDS: CO_2 sequestration, magnesium silicate, mineral carbonation

INTRODUCTION

The volume of carbon dioxide associated with the use of fossil fuels to produce electricity is enormous. For example, in the United States alone, ~1.8 Gtons of CO_2 was emitted in 1999, and for comparison, water withdrawn in 1990 in the U. S. for public supplies was ~55 Gtons. The scale of CO_2 production is central to any viable method to store captured CO_2 in order to reduce emissions. Consequently, most methods being considered as options for CO_2 storage exploit one of the major natural carbon reservoirs, such as the oceans, subsurface reservoirs (such as brines or depleted oil & gas fields), or the terrestrial carbon pool. Related to subsurface reservoirs are carbonate rocks, which are the dominant natural pool for oxidized carbon. Carbonate rocks develop largely from the interaction of aqueous fluids with silicate rocks enriched in calcium and magnesium, either through weathering, ground water flow, or hydrothermal activities: each of these fluid–rock interactions can lead, essentially, to the release of the alkaline-earth metals from the silicates via dissolution, leaching, or other mineral-alteration reactions. Once released to the aqueous fluid, the alkaline-earth metals can react with dissolved CO_2 to precipitate carbonates. The net result is the conversion of carbon dioxide to a thermodynamically stable and immobile form.

Seifritz (1990) proposed exploiting this natural process as a means for storing CO_2 captured from the burning of fossil fuels. Lackner et al. (1995) explored this concept in the context of an industrial carbonation process and suggested that magnesium silicates (derived from ultramafic rocks) would provide an abundant and thermodynamically convenient resource for the production of magnesium carbonate (specifically, magnesite, $MgCO_3$). Lackner et al. (1995) and Goff and Lackner (1998) showed that the economics of using ultramafic rocks for carbonation and their abundance are compatible with the scale of CO_2 storage. The primary global magnesium sources, as noted by Goff and Lackner (1998), are the minerals of the olivine group (e.g., forsterite) and serpentine group, which carbonate by the overall reactions:

$$Mg_2SiO_4 + 2CO_2 \Rightarrow 2MgCO_3 + SiO_2 \quad (1)$$
(forsterite) (magnesite)

$$Mg_3Si_2O_5(OH)_4 + 3CO_2 \Rightarrow 3MgCO_3 + 2SiO_2 + 2H_2O \quad (2)$$
(serpentine)

These reactions represent the general concept of mineral carbonation as envisaged by Lackner and coworkers.

One of the principal challenges to making this process work industrially is to develop an economic and rapid method for extracting the magnesium from the rock. Wendt et al. (1998a,b,c) investigated the use of a molten salt process for producing magnesium hydroxide from magnesium silicate. (Magnesium hydroxide carbonates readily.) The method is rapid but involves corrosive conditions that create materials issues that must be addressed prior to an industrial implementation. Several other processes have also been suggested as potential routes for industrial carbonation of ultramafic rocks, including carbonation in an aqueous medium (O'Connor et al., 2000), direct carbonation in supercritical CO_2, and various multi-step processes (e.g., Lackner et al., 1997). Carbonation in an aqueous medium shows potential for being able to achieve needed carbonation rates in a relatively simple chemical process, but it presents the challenge of achieving carbonation rates that are economic and matched to the scale of CO_2 generation rates (on the order of (5×10^3 mol CO_2/sec for a 1 GWatt plant). This challenge is the focus of an intensive research effort by the DOE-funded Mineral Carbonation Research Cluster, which consists of researchers at Los Alamos National Laboratory, Albany Research Center, Arizona State University, National Energy Research Laboratory, and Science Applications International Corporation. We are attempting to solve this challenge in an experimental system that is a bench scale version of what we anticipate for the industrial process: a stirred reaction vessel (autoclave) that can operate at elevated temperatures and pressures. (We typically operate at T up to 185°C and P up to ~2300 psi, with ~0.8 litre of water+solids and ~1 litre of supercritical CO_2 in the vessel.)

In this paper, we outline a geochemical model for the carbonation of magnesium silicates in a two-fluid system. The model is consistent with our experimental system and with potential industrial processes that could develop from our current efforts on aqueous carbonation of serpentine and olivine. A parallel to carbonation of ultramafic rocks in an industrial setting would rely on carbonation of similar minerals *in situ* following emplacement of a CO_2 plume in a suitable geological reservoir. The geochemical model we outline below is compatible with this type of environment as well. Advantages of mineral carbonation have been detailed in numerous other papers, including Lackner et al. (1995) and a paper in this volume Goldberg et al. (2001; this conference).

THE BASIC GEOCHEMICAL MODEL

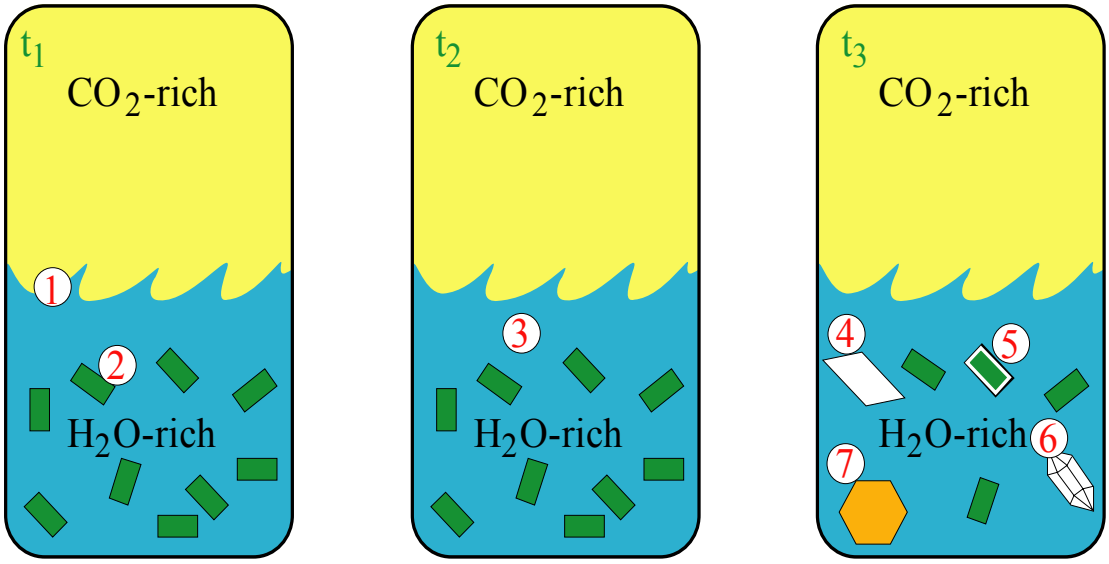

Figure 1. Schematic representation of geochemical processes occurring at different time points (t_1, t_2, t_3) in the process: 1) The dissolution of CO_2 into the aqueous medium and H_2O into the supercritical CO_2; 2) dissolution of the Mg-silicate into the aqueous medium; 3) speciation of the aqueous fluid in response to the dissolution of CO_2 and of the Mg-silicate; and 4) precipitation of a carbonate phase. Additional phenomena might include development of a leached layer or surface precipitate on the dissolving particle (5), precipitation of silica phases (6), and precipitation of phases of iron and other minor/trace elements (7).

The basic geochemical model is outlined schematically in Figure 1. As shown, the model makes two assumptions. First, the model assumes dissolution and precipitation phenomena occur in the aqueous phase and not in the supercritical CO_2 phase. The second assumption is that the carbonation process occurs dominantly via dissolution–precipitation and not by direct carbonation of the Mg-silicate. In the case of our experimental efforts (e.g., O'Connor et al., 2000; Ziock et al., unpublished data and as reported in this paper), we believe both of these assumptions to be appropriate.

In our experimental system, density arguments support the first assumption. Although the system is agitated by a rotating propeller, the rotation rates used are believed to be insufficient to mix the system completely (leaving the system stratified with the denser aqueous fluid and particles at the bottom). In addition, water is believed to be the favored wetting phase for hydrophilic solids. Unfortunately, no comprehensive data are available on the surface thermodynamics of serpentine, but one study suggests chrysotile is moderately hydrophobic (Giese and van Oss, 1993), implying supercritical CO_2 may be a better wetting phase. This latter argument becomes important in natural systems where density stratification does not determine partitioning.

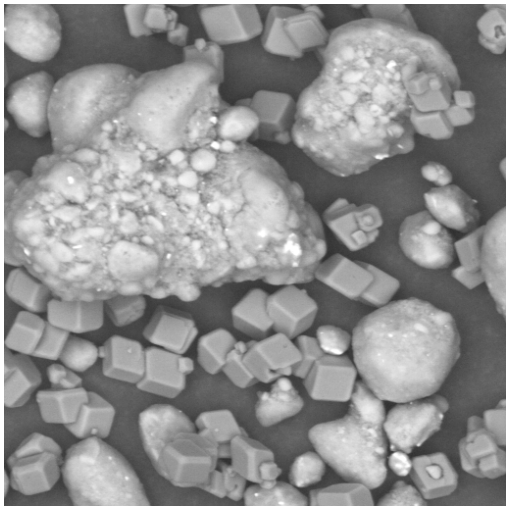

Figure 2. Secondary electron image of run products from LANL experiment 41300, showing rhombohedral magnesite crystals and rounded particles of serpentinite. Image is approximately 200 μm across. Sample was from an experiment in which the serpentine lizardite (heat treated at 630°C for 2 hrs; bulk powder has 80 wt% passing a 320 mesh sieve) was exposed in a stirred autoclave (Parr Instruments) to an aqueous solution of sodium bicarbonate (0.64*M*) and sodium chloride (1*M*) for 5.25 hrs at *T*=195°C and P_{CO2}~129 atm. Run products consisted of the original heat treated serpentine and magnesite (21 wt%) as determined directly by quantitative X-ray diffraction methods.

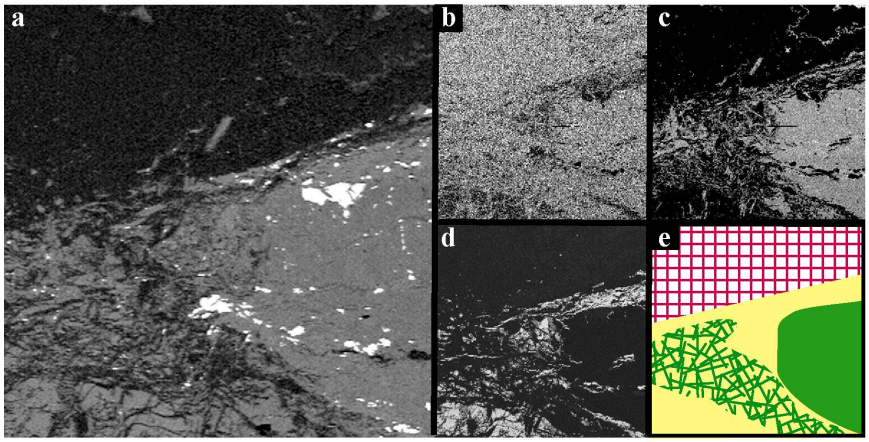

Figure 3. Scanning electron microscope images of a polished cross section through a carbonate vein within an altered serpentinite, Delight Quarry, MD. (a) Back-scattered electron image showing magnetite crystals (bright) within an unaltered serpentine rich area (gray on right side), vein magnesite and calcite (both dark) with minor silica (gray stringers) and zones of discrete carbonate and serpentine. (b) Mg X-ray map of region. (c) Si X-ray map showing, distribution of serpentine (co-location of Mg and Si). (d) Ca X-ray map showing distribution of Ca-carbonate alteration. (e) Sketch showing mineral zones, solid green showing original serpentine, solid yellow Ca carbonate alteration, stippled green-yellow serpentine+carbonate, and hatched area magnesite.

The second assumption is supported by scanning electron microscopy images of our experimental run products (Fig. 2), which show discrete carbonate crystals forming

separated from the silicate particles. O'Connor and coworkers report similar observations for olivine exposed under similar experimental conditions. Although these images do not rule out some carbonation occurring directly on or within Mg-silicate particles (e.g., as reported by Lackner et al., 1997 and McKelvy and coworkers, for gas–solid carbonation of brucite), they do demonstrate that a large portion (if not all) of the Mg is precipitated separate from the silicates. Similar textures can be observed in natural systems in which magnesium carbonate typically forms physically separated from the silicates (Fig. 3; Goff and Guthrie, 1999; Goff et al., 2000).

Returning to the geochemical model in Figure 1, four steps must occur during the conversion of CO_2+serpentine into solid magnesium carbonate: carbon dioxide must dissolve into the aqueous phase (and vice versa) (step #1); magnesium must dissolve into the aqueous phase (step #2); the aqueous phase must speciate in response to dissolved components, *T*, *P*, etc. (step #3); and magnesium carbonate (ideally magnesite) must precipitate (step #4). Although these steps may actually consist of multiple steps, they represent in a general sense the phenomena that occur during aqueous carbonation. Additional phenomena depicted in Fig. 1 include possible changes in the nature of dissolution of the Mg-silicate (e.g., congruent or incongruent, #5) and the fate of silica (#6) and minor and trace metals, particularly iron (#7).

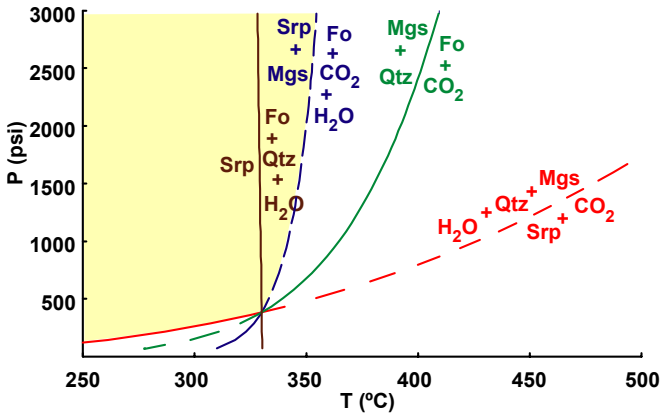

Figure 4. Calculated equilibrium *P*–*T* relationships in the system MgO–SiO_2–H_2O–CO_2 for the phases magnesite (Mgs), quartz (Qtz), the serpentine chrysotile (Srp), forsterite (Fo), water (H_2O), carbon dioxide (CO_2), and for P_{H2O}=250 psi. P_{total} was set to P_{CO2}+P_{H2O}. Calculations were done using the thermodynamic data from Robie and Hemingway (1995) and the equation of state for CO_2 from Duan et al. 1992). Dashed lines indicate regions where the reaction is metastable relative to the invariant point. Yellow area shows *P*–*T* region in which magnesite can be formed from forsterite or serpentine.

Both thermodynamic and kinetic factors constrain the conditions under which the carbonation of Mg-silicates will occur at rate practical for an industrial process. Figure 4 shows calculated thermodynamic relationships around the invariant point involving the phases under discussion. The reactions shown in red and green represent the carbonation of serpentine (chrysotile) and forsterite, respectively. These reactions occur at relatively high temperatures, implying in the case of serpentine, for example, that carbonation should occur at temperatures up to ~400°C for P_{CO2} over ~1000 psi. The conditions are

somewhat more restrictive, however, due to other reactions in the multiphase system. For example, serpentine is not stable in the presence of magnesite at temperatures above ~350°C but will react to form forsterite, restricting the *P–T* of carbonation to *T*<~350°C (i.e., the shaded yellow region in Fig. 4).

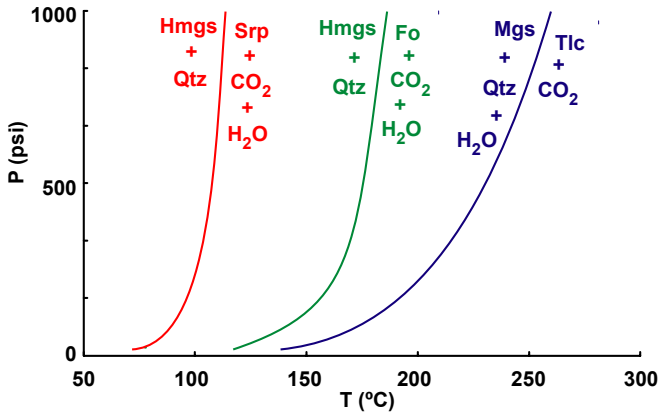

Figure 5. Calculated *P–T* relationships in the system MgO–SiO_2–H_2O–CO_2 showing the carbonation reaction for talc (Tlc) and magnesite and the hydrocarbonation reactions converting chrysotile or forsterite into hydromagnesite (Hmgs), $Mg_5(OH)_2(CO_3)_4{\cdot}4H_2O$. Calculations were done using the thermodynamic data from Robie and Hemingway (1995), for P_{H2O}=250 psi (with P_{total} set to P_{CO2}+P_{H2O}), and using the equation of state for CO_2 from Duan et al. 1992).

Carbonation conditions may be significantly more restrictive when one considers equilibria involving other phases in the system, such as talc, or other reaction paths, such as via hydromagnesite. Figure 5 shows the carbonation reaction involving talc ($Mg_3Si_4O_{10}(OH)_2$). Talc will react with CO_2 at *T*<250°C at P_{CO2}<~750 psi. Conversely, the assemblage magnesite+quartz+H_2O is unstable at T>250°C (P_{H2O}=250psi) relative to talc+CO_2. This reaction may limit the carbonation of serpentine or forsterite to *T*<250°C, although precipitation of talc is likely to be inhibited kinetically under these conditions.

More important constraints on the carbonation conditions of serpentine and forsterite may derive from the other two reactions in Figure 5. Many studies have reported that direct nucleation and growth of magnesite can be slow such that magnesite may typically form by carbonation of hydromagnesite, which forms more rapidly under aqueous conditions (e.g., Möller, 1989). If this carbonation mechanism is the dominant route, then forsterite carbonation may be limited to *T*<~175°C at *P*=1000 psi and serpentine carbonation may be limited to *T*<~120°C at *P*=1000 psi.

Ultimately, the rate of reaction will be a critical factor in determining whether an aqueous carbonation process can be used to convert CO_2 into a solid on an industrial scale. The rate of the reaction will depend on the slowest step(s) in the geochemical conceptual model of Figure 1. Each of these steps will be evaluated in the next few sections.

EQUILIBRATION OF THE CO_2–H_2O FLUIDS

In the H_2O-CO_2 system, thermodynamic relationships are not precisely known, due to discrepancies in the experimental data. However, in general, over the *P–T* range we're

investigating, water contents greater than about 5–10 mole% will result in two fluids: an aqueous fluid with ~5–10 mole% CO_2, and a supercritical carbon dioxide fluid with a significant H_2O content.

Most of the uncertainty lies in the H_2O contents of the carbon dioxide fluid as opposed to the CO_2 contents of the aqueous fluid. The nature of H_2O in the carbon-dioxide-rich fluid may impact the aqueous fluid indirectly through desiccation, which in turn impacts the activities of the aqueous species. (Desiccation occurs as the water leaves the aqueous phase and partitions into the supercritical CO_2 phase.) The principal rate-controlling factors related to the equilibration of the two fluids are the diffusion of CO_2 across the fluid–fluid interface into the aqueous medium (and vice versa) and the formation of carbonic acid (i.e., $H_2O+CO_2=H_2CO_3$). Although it is tempting to think that this step would not be rate controlling relative to other processes in our experimental system, one explanation posited for the experimental discrepancies alluded to above is that the system takes a long time (up to 24 hrs) to equilibrate. Nevertheless, most of the slow equilibration involves the CO_2 fluid and not the aqueous fluid, which means its impact on the carbonation process is limited to the desiccation phenomenon mentioned above. One study in support of CO_2 dissolution into the aqueous phase as a rate limiting step is that reported by Smithson and Bakhshi (1973) who found this step to be rate limiting for carbonation of MgO slurries at 38°C but not at $T \leq 28$°C. This study is not directly relevant to carbonation of Mg silicates, because of the much faster dissolution rate for MgO (as seen below). In other words, dissolution for silicates is so much slower that it is likely to impact carbonation rate more than it would for MgO.

MINERAL DISSOLUTION: RELEASE OF MG TO THE AQUEOUS PHASE

The release of magnesium to the aqueous fluid is likely to be an important rate-limiting step in the carbonation process. Surface sites on particles of forsterite and serpentine may release Mg^{2+} rapidly via a cation exchange process. However, the structure of neither silicate is amenable to rapid cation diffusion at low temperatures, so cation exchange will be minor. The bulk of the Mg^{2+} must be released by a dissolution process. Salts typically dissolve congruently, releasing stoichiometric amounts of constituents. However, many silicates initially dissolve incongruently, typically leaving a layer enriched in alumina (if present) and silica but depleted in alkalis and alkaline earths. Indeed, many studies of the dissolution of serpentines report an initial stage of incongruent dissolution with the development of a silica layer on the particle surfaces, followed by congruent behavior as dissolution proceeds. A silica layer has also been observed on particles of forsterite recovered from carbonation runs (O'Connor, pers. comm.). The degree of congruent behavior for dissolution can be determined by evaluating whether the concentration profiles have the stoichiometry of the dissolving mineral.

The concentration profile also reveals whether the dissolution mechanism is controlled by diffusion or surface phenomena. Two end-member cases for describing the rate of mineral dissolution are transport-limited and surface-limited, for which the concentration of a dissolved species (C) varies either as $t^{0.5}$ or t^{1}, respectively (Stumm and Morgan, 1996):

$$\text{Rate} = \frac{dC}{dt} = k_p\, t^{-0.5} \qquad (3a)$$

which by integration gives

$$C = C_0 + 2 k_p t^{0.5} \quad (3b)$$

where k_p is the reaction rate constants (in units of mol-sec$^{-0.5}$), t is time (seconds), A is the reactive surface area (m^2). (The term $k_{P,T,X}$ is normally written as simply k; however, the subscript is used here to stress that this reaction rate is dependent on the state of the system, i.e., it is dependent on pressure, temperature, and composition of both the solids and fluids.)

In the transport-limited (diffusion controlled) case, the surface processes (e.g., attachment of protons or complexing ligands) are so rapid that dissolution becomes limited by the diffusion of a dissolving species through a surface layer. Another factor that can lead to transport-limited dissolution is incongruent dissolution, whereby a surface layer (e.g., a leached layer or a precipitated layer) forms on the outside of a dissolving particle.

A general kinetic description for heterogeneous mineral-surface processes is given by Lasaga (1995):

$$\text{Rate} = k_0 \, A \, e^{-\text{Ea/RT}} \, g(\text{I}) \, \Pi \left(a_{sp}^{n_{sp}}\right) \, f(\Delta G_r) \quad (4)$$

where k_0(mol m^{-2} sec^{-1}) is the rate constant, A(m^2) is the reactive surface area, $e^{-\text{Ea/RT}}$ accounts for affects due to activation energy and temperature, g(I) accounts for the dependence of rate on ionic strength of the solution, $\Pi \left(a_{sp}^{n_{sp}}\right)$ is the product of the activities of aqueous species (*e.g.*, H^+) that impact rate for a given order n_{sp} (e.g., n=1 is a first-order affect), and $f(\Delta G_r)$ defines the dependence of rate on deviation from thermodynamic equilibrium. As noted by Lasaga, each of the effects is multiplicative. Also, as noted by Lasaga, A is reactive surface area, which is not necessarily equivalent to surface area. The meaning of and measurement of reactive surface area is highly debated.

By comparing Eq. 3 and Eq. 4, it is easy to see that the rate constants are related as follows:

$$k_{P,T,X} = k_0 \, e^{-\text{Ea/RT}} \, g(\text{I}) \, \Pi \left(a_{sp}^{n_{sp}}\right) \, f(\Delta G_r) \quad (5)$$

In other words, a k that is typically reported in the literature will be $k_{P,T,X}$ for a specific set of conditions, and the dependence of k on these other factors must be known to extrapolate the k value to a different set of conditions. For some of these factors, educated guesses can be made (e.g., the use of an average value for E_a for a mineral for which the activation energy is not known). Others (e.g., the dependence of k on pH) must be determined experimentally. The factor $f(\Delta G_r)$ is effectively a dampening term that is unity at very dilute conditions and becomes smaller as saturation is approached. Hence, setting this factor to 1 provides a best-case estimate of the dissolution rate.

In addition to the factors embedded in the rate constant, there are a number of other variables that are important in dissolution rate. As shown in Eq. 4 and discussed above, reactive surface area is directly proportional to dissolution rate in a surface-limited situation. Although it is distinct from surface area as measured by a technique such as BET, reactive surface area is likely to be related to overall surface area. Hence, increasing overall surface area should increase reactive surface area.

From an anecdotal perspective, Mg-oxides and hydroxides—e.g., periclase (MgO) and brucite—carbonate relatively rapidly under the conditions we've been investigating,

whereas olivine and serpentine carbonate more slowly. Dissolution rates for these phases at 25°C are typically ~10^{-5}–10^{-6} mol/m^2/sec (brucite and periclase), ~10^{-10}–10^{-11} mol/m^2/sec (serpentine and olivine), in other words they are consistent with dissolution playing a role in determining carbonation rate. If dissolution is the rate-limiting step, then it controls carbonation rates.

We have been investigating the dissolution rates of our serpentine samples to determine the dissolution rates of our materials and to test various methods for enhancing the dissolution rate. Dissolution experiments were conducted in batch mode in deionized water at ~60°C stirred with a floating magnetic stir bar; initial experiments were open to the atmosphere, allowing some CO_2 into the system. Current experiments are also investigating dissolution under controlled atmospheres.

Our preliminary data are consistent with dissolution rates playing an important role in carbonation. Figure 6 shows the dissolution behavior for a forsterite and serpentine (lizardite) at 60°C. The serpentine sample apparently dissolved incongruently under these conditions, with Mg:Si = 0.6 as opposed to the stoichiometric value of 1.5. As noted above, serpentine typically dissolves incongruently but with Mg:Si greater than ideal. This atypical behavior of our serpentine has been reported for a lizardite dissolved under similar pH conditions by Luce et al. (1972); we are currently attempting to determine the cause of this behavior: The initial rate of dissolution for the serpentine sample was 1.5×10^{-10} mol/m^2/sec slowing to a rate of 1.2×10^{-11} mol/m^2/sec (based on Mg release).

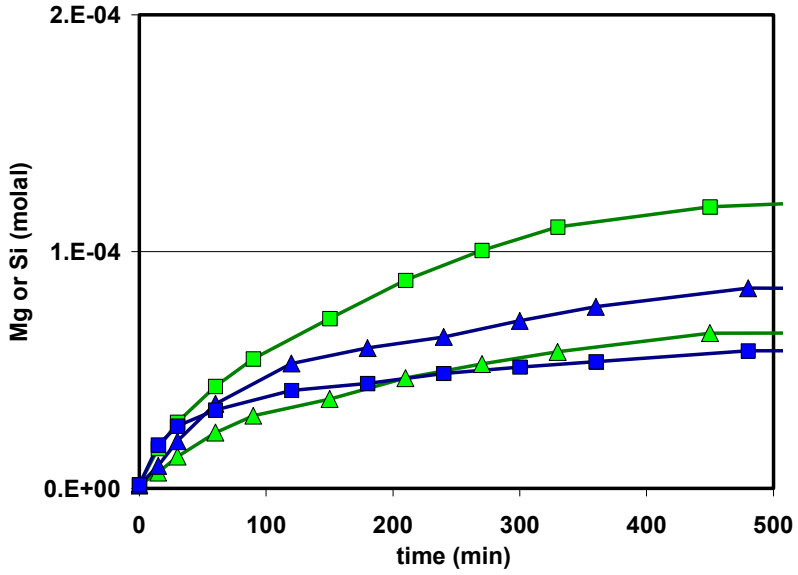

Figure 6. Dissolution characteristics of an olivine and serpentine (lizardite) sample in a batch aqueous process. Blue boxes and triangles show the Si and Mg concentrations (respectively) for a forsteritic olivine (LANL-HMOL18-5); green boxes and triangles show the Si and Mg concentrations (respectively) for a lizardite sample (LANL-UN9801-F23).

The olivine sample also dissolved incongruently, with an initial Mg:Si of 0.5 (ideal = 2) steadying at 1.4 as dissolution proceeded. The initial rate of dissolution for olivine

was 5×10^{-10} mol/m^2/sec slowing to 8×10^{-11} mol/m^2/sec. Hence, the rate for olivine dissolution was higher than that for serpentine by about a factor of 3–5. In addition, Figure 6 shows that that amount of Mg released in the olivine dissolution exceeded the amount in the lizardite dissolution by a factor of ~1.5. With respect to carbonation, the forsterite sample carbonates slightly faster than the lizardite at 155°C.

Figure 7 shows the same dissolution data for the serpentine (green) and the dissolution data for heat-treated serpentine (treated at 630°C). (The heat treated sample carbonates much more rapidly than the non-heat-treated sample.) The initial rate of dissolution for the heat-treated sample was 3.5×10^{-9} mol/m^2/sec slowing to a rate of 2×10^{-11} mol/m^2/sec (based on Mg release). Interestingly, the stoichiometry for the dissolution of the heat-treated material was close to stoichiometric at the start of dissolution (~1.6–1.7) but became incongruent at later stages, where the ratio was more typical of what is observed for serpentine (Mg:Si = 2–3). Hence, the dissolution rate for heat-treated serpentine was much higher than that for the original serpentine by about a factor of 2–20. In addition, Figure 7 shows that that amount of Mg released in the dissolution of heat-treated serpentine exceeded the amount released by the original serpentine by a factor of ~7.

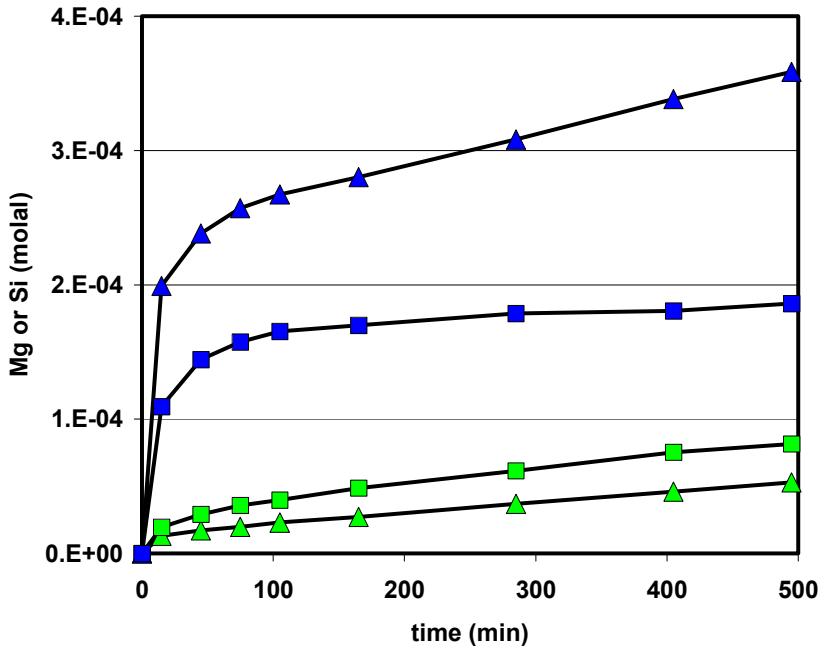

Figure 7. Dissolution characteristics of a serpentine (lizardite) and heat-treated serpentine sample in a batch aqueous process. Blue boxes and triangles show the Si and Mg concentrations (respectively) for heat-treated serpentine (LANL-HT1), which was heated to 630°C for 10 hrs in CO_2; green boxes and triangles show the Si and Mg concentrations (respectively) for a lizardite sample (LANL-UN9801-F23).

SPECIATION OF THE AQUEOUS PHASE

The state of the aqueous fluid will have a major impact on the carbonation process in a number of ways. As discussed above, dissolution of CO_2 into the aqueous fluid is a critical step in the carbonation process that can be described by a series of steps:

$$CO_{2(gas)} \Rightarrow CO_{2(aq)} \quad (6)$$

$$CO_{2(aq)} + H_2O \Rightarrow H_2CO_3 \quad (7)$$

$$H_2CO_3 \Rightarrow H^+ + HCO_3^- \quad (8)$$

$$HCO_3^- \Rightarrow H^+ + CO_3^{2-} \quad (9)$$

These reactions will have a major impact on pH (but not the only impact). In addition, they determine the concentration of aqueous carbonate (CO_3^{2-}) that is present, which impacts the solubility of solid carbonate through the reaction:

$$Mg^{2+} + CO_3^{2-} \Rightarrow MgCO_3 \quad (10)$$

The distribution of CO_2 among the various species in Eqs. 6–9 is determined by pH. In general, at low pH, H_2CO_3 (carbonic acid) dominates; at mid pH, HCO_3^- (bicarbonate) dominates; at high pH, CO_3^{2-} (carbonate) dominates. Under the conditions that are most likely present during our experiments, bicarbonate and perhaps carbonic acid dominate.[¥]

Speciation of the fluid is also an important factor, because it determines the amount of solute required for each solid phase to be saturated—i.e., it will determine how much a mineral will dissolve before Mg carbonate will precipitate. Speciation is a function of the entire system, which means that many of the equilibria are interdependent and must be solved simultaneously. There are a number of geochemical computer codes that can provide information on the speciation of the fluid under our conditions. Thermodynamic descriptions of many of the species of concern are available; however, as noted above, the description of the CO_2–H_2O system (particularly when solutes are present) is not well described. This uncertainty will impart an uncertainty to any thermodynamic calculations, because all of the aqueous species will depend in part on the nature of CO_2 in the fluid.

Ionic strength— $^1/_2\ \Sigma c_i Z_i^2$, where c_i and Z_i are the concentration and charge for each aqueous species *i*—impacts a variety of processes in our system. As discussed above, ionic strength can play a role in the rate of mineral dissolution (Eq. 4). For example, Dove (1995) discusses the transition state theory that explains the enhancement of silica dissolution by the presence of sodium ion, which is reflected in part in the positive effect of ionic strength on rate. (The activity term in Eq. 4 also accommodates this effect.) Ionic strength comes into play indirectly in the dissociation energy associated with breaking the hydration sphere of Mg^{2+}, which is a necessary step in the formation of $MgCO_3$. However, breaking this sphere may not be as important in the formation of hydromagnesite—$(MgCO_3)_4Mg(OH)_2{\bullet}4H_2O$.

The kinetics of the equilibria in Eqs. 6–9 are discussed by Stumm and Morgan (1996). At room T, Eq. 7 is rate limiting and first order with respect to $CO_{2(aq)}$, but it requires only minutes to reach steady state. In contrast, as discussed above, experimental

---

[¥] The speciation of CO_2 was based on equilibrium preliminary reaction-path, thermodynamic calculations that estimated the evolution of pH in a system of aqueous fluid reacting with serpentine with an excess CO_2 pressure.

studies of the CO_2–H_2O system have suggested that equilibration may take hours, suggesting that Eq. 6 may be rate limiting for carbonate equilibria in a two-fluid system.

Speciation of the fluid generally occurs rapidly, particularly for low valence ions (Stumm and Morgan, 1996). Hence, this step is not likely to be rate-limiting in our system.

CARBONATE PRECIPITATION

A number of carbonate-bearing Mg phases can occur at low *T*, including magnesite, hydromagnesite, nesquehonite, artinite, and lansfordite. In general, magnesite is stable at higher temperatures, but other carbonate phases can be kinetically favored as the initial Mg carbonate formed. These metastable carbonates can convert to magnesite over time, as has been observed experimentally. One of the thermodynamic barriers to magnesite formation is the activation energy associated with disrupting the hydration sphere of Mg^{2+}. Consequently, partially hydrated carbonates may form more readily from an aqueous solution. Indeed, as noted by Möller (1989), magnesite precipitation experimentally typically proceeds via a hydromagnesite precipitation initially followed by carbonation of the hydromagnesite to form magnesite, which occurs at elevated *T* or P_{CO2}. As shown by the thermodynamic calculations in Figs. 4–5, the mechanism by which the carbonate forms (i.e., magnesite directly or indirectly) has a big impact on the maximum temperature for the carbonation reaction. One option is to allow the CO_2 to be stored as a hydrated carbonate (such as hydromagnesite). However, two disadvantages to this approach are the relative instability of hydromagnesite as a permanent sink for CO_2 and the dramatically increased solid mass and volume per mole of CO_2 sequestered. This latter aspect has big negative impacts on the cost and feasibility of disposal.

We are currently investigating the precipitation mechanisms responsible for carbonation of serpentine in our system. Although the final product we produce is typically magnesite, hydromagnesite has been formed in several runs in which the fluid chemistry was altered or in which the CO_2 was vented from the autoclave prior to quenching.

CONCLUSIONS

During aqueous carbonation of Mg silicates, there are likely to be four basic steps that could impact the rate. These include dissolution of CO_2 into the aqueous phase, dissolution of the silicate to release Mg, speciation of the fluid components, particularly the carbonic acid, and precipitation of the carbonate. We have been investigating several of these steps, including dissolution rates and mechanisms. The order of dissolution rates appear to parallel the order of carbonation rates, implying that dissolution plays an important role. In addition to the four steps described, other factors that must be addressed en route to developing a feasible carbonation process include the fate of silica and minor/trace metals like iron. Silica in particular may be important in impacting the carbonation rate and mechanism, by forming a silica enriched layer on the dissolving particles over time, changing the rate and mechanism of dissolution. The fate of silica is an important factor being addressed by the Mineral Carbonation Research Cluster.

REFEENCES

Bish, D. L. and Post, J. E. (1993) Quantitative mineralogical analysis using the Rietveld full pattern fitting method. *American Mineralogist*. **78:**932–940.

Dove, P. M. (1995) Kinetic and thermodynamic controls on silica reactivity in weathering environments. In: *Chemical Weathering Rates of Silicate Minerals*, Rev. in Mineralogy, v. 31, White, A. F. and Brantley, S. L. (eds.), Mineralogical Soceity of America, Washington, 235–282.

Duan, Z., Møller, N., and Weare, J. H. (1992) An equation of state for the CH4-CO2-H2O system.2. Mixtures from 50°C to 1000*C and 0 to 1000 bar. *Geochem. Cosmochim. Acta,* **56:**2619–2631.

Giese, R. F., Jr. and van Oss, C. J. (1993) The surface thermodynamic properties of silicates and their interactions with biological materials. In: *Health Effects of Mineral Dusts*, Rev. in Mineralogy, v. 28, Guthrie, G. D., Jr. and Mossman, B. T. (eds.), Mineralogical Society of America, Washington, 327–346.

Goff, F., and Guthrie, G., (1999) Field trip guide to serpentinite, silica-carbonate alteration, and related hydrothermal activity in the Clear Lake region, California: Los Alamos Nat. Lab., Report. LA-13607-MS, 29 pp.

Goff, F., and Lackner, K. S., (1998) Carbon dioxide sequestering using ultramafic rocks: *Environmental Geosciences*, **5:**89–101.

Goff, F., Guthrie, G. D., Lipin, B., Fite, M., Chipera, S. J., Counce, D. A., Kluk, E., and Ziock, H. (2000) Evaluation of Ultramafic Deposits in the Eastern United States and Puerto Rico as Sources of Magnesium for Carbon Sequestration. Los Alamos Nat. Lab., Report. LA-13693-MS, 30 pp.

Lackner, K.S., Wendt, C. H., Butt, D.P., Joyce, E.L., and Sharp, D.H. (1995) Carbon dioxide disposal in carbonate minerals: *Energy* **20:**1153–1170.

Lackner, K. S., Butt, D. P., Wendt, C. H. (1997) Progress on binding CO_2 in mineral substrates. *Energy Conversion Management*, **38:**S259–S264.

Lasaga, A. C. (1995) Fundamental approaches in describing mineral dissolution and precipitation rates. In: *Chemical Weathering Rates of Silicate Minerals*, Rev. in Mineralogy, v. 31, White, A. F. and Brantley, S. L. (eds.), Mineralogical Society of America, Washington, 23–86.

Luce, R. W., Bartlett, R. W., Parks, G. A. (1972) Dissolution kinetics of magnesium silicates. *Geochim. Cosmochem. Acta*, **36:**35–50.

Möller, P. (1989) Nucleation processes of magnesite. *Mineral Deposits*, **28:**287–292.

O' Connor, W.K., Dahlin, D. C., Nilsen, D. N., Walters, R. P., and Turner, P. C. (2000) Carbon Dioxide Sequestration by Direct Mineral Carbonation with Carbonic Acid. *Proceedings, 25th International Technical Conference on Coal Utilization and Fuel Systems*, Coal Technology Association, Clearwater, Florida.

Robie, R. A. and Hemingway, B. S. (1995) Thermodynamic properties of minerals and related substances at 298.15K and 1 bar (10^5 Pascals) pressure and at higher temperatures. U. S. Geological Survey Bulletin 2131, 461 p.

Seifritz, W. (1990) CO_2 disposal by means of silicates.*Nature* **345**:486.

Smithson, G. L. and Bakhshi, N. N. (1973) Kinetics and mechanism of carbonation of magnesium oxide slurries. *Ind. Eng. Chem. Process Des. Develop.*, **12:**99–106.

Stumm, W. and Morgan, J. J. (1996) Aquatic Chemistry. John Wiley and Sons, New York, 1022 p.

Wendt, C. H., Butt, D. P., Lackner, K. S., and Ziock, H.-J. (1998) Thermodynamic calculations for acid decomposition of serpentine and olivine in MgCl2 melts, 1: description of concentrated MgCl2 melts. Los Alamos Nat. Lab., Report. LA-984528, 23 pp.

Wendt, C. H., Butt, D. P., Lackner, K. S., and Ziock, H.-J. (1998) Thermodynamic calculations for acid decomposition of serpentine and olivine in MgCl2 melts, 2: reaction equilibria in MgCl2 melts. Los Alamos Nat. Lab., Report. LA-984529, 29 pp.

Wendt, C. H., Butt, D. P., Lackner, K. S., Vaidya, R. U., and Ziock, H.-J. (1998) Thermodynamic calculations for acid decomposition of serpentine and olivine in MgCl2 melts, 3: heat consumption in process design. Los Alamos Nat. Lab., Report. LA-985633, 24 pp.